Since January 2020 Elsevier has created a COVID-19 resource centre with free information in English and Mandarin on the novel coronavirus COVID-19. The COVID-19 resource centre is hosted on Elsevier Connect, the company's public news and information website.

Airflow and droplet spreading around oxygen masks: A simulation model for infection control research

Margaret Ip, FRCPath,[a,b] Julian W. Tang, MRCPath,[b] David S. C. Hui, FRCP,[a,c] Alexandra L. N. Wong, PhD,[a,d] Matthew T. V. Chan, FCCP,[e] Gavin M. Joynt, FCCP,[e] Albert T. P. So, PhD,[d] Stephen D. Hall, PhD,[f] Paul K. S. Chan, FRCPath,[b] and Joseph J. Y. Sung, FRCP[a,c]
Hong Kong, China, and Sydney, Australia

Background: Respiratory assist devices, such as oxygen masks, may enhance the potential to spread infectious aerosols from patients with respiratory infections.
Methods: A technique was developed to visualize exhaled aerosols during simulated patients' use of oxygen masks in a health care setting and tested using the simple, the nonrebreathing, and the Venturi oxygen masks. A smoke tracer was introduced into one of the lungs of the model to enable it to mix with the incoming oxygen and then to be further inhaled/exhaled by the model according to a variety of realistic respiratory settings (14, 24, and 30 breaths per minute, with tidal volumes of 500, 330, 235 mL, respectively) and oxygen supply flow rates (between 6 and 15 liters per minute). Digital recordings of these exhaled airflow patterns allowed approximate distances to be estimated for the extent of the visible exhaled air plumes emitted from each oxygen mask type at these settings.
Results: It was found that the simple, the nonrebreathing, and the Venturi-type oxygen masks produced exhaled smoke plumes over minimum distances of 0.08 to 0.21 m, 0.23 to 0.36 m, and 0.26 to 0.40 m, respectively.
Conclusion: Health care workers may therefore consider any area within at least 0.4 m of a patient using such oxygen masks to be a potential nosocomial hazard zone. (Am J Infect Control 2007;35:684-9.)

Since the 2003 severe acute respiratory syndrome (SARS) outbreaks, there has been an increased interest in aerosol transmission of infectious agents. Several reviews and studies discussing the potential for aerosol transmission of various infectious agents have since been published,[1,2] including those on SARS-associated coronavirus,[3-12] varicella zoster virus (causing chickenpox),[12] tuberculosis,[13] and influenza.[14-16] Others have studied the potential for health care procedures to act as generators or amplifiers of sources of infection, particularly the use of oxygen masks and ventilation methods.[17-19]

From the Centre for Emerging Infectious Diseases, School of Public Health,[a] Department of Microbiology,[b] and Department of Medicine and Therapeutics,[c] The Chinese University of Hong Kong, Shatin, New Territories; Department of Building and Construction,[d] City University of Hong Kong, Kowloon, Hong Kong SAR, China; Department of Anaesthesia and Intensive Care,[e] The Chinese University of Hong Kong, Shatin, New Territories, Hong Kong SAR, China; and School of Mechanical Engineering,[f] University of New South Wales, Sydney, Australia.

Address correspondence to Julian W. Tang, MRCPath, Department of Microbiology, Chinese University of Hong Kong, Prince of Wales Hospital, Shatin, New Territories, Hong Kong SAR, China. E-mail: julian.tang@cuhk.edu.hk.

Supported by the Research Fund for the Control of Infectious Diseases (RFCID) from the Health, Welfare, and Food Bureau of the Hong Kong SAR government (grant No. CUHK-CS-002; to project team).

0196-6553/$32.00

doi:10.1016/j.ajic.2007.05.007

Visualization of airflows is difficult, and recent techniques have involved the use of tracer particles of nebulized liquid droplets in a cloud[17] or solid particulates in a smoke.[18,19] Furthermore, the quantitative analysis of such suspended liquid or solid particles is difficult because it depends, ultimately, on their visibility on the recorded image. Although the movement of these tracer particles may follow the airflow movements precisely,[18-21] the exhaled liquid (including mucous) droplets from a potentially infected patient will probably not do so, especially because evaporation will be continuously changing its size and mass.[2,22] Such limitations notwithstanding, the visualization of exhaled air plumes from oxygen masks in health care settings is still useful for planning the control of potentially infectious aerosols, not only for a possible influenza pandemic but for daily encounters with tuberculosis (TB), measles, and chickenpox in hospitals and other health care and community environments. Here, we present some estimates of dispersal distances of smoke-visualized airflows produced using a realistic lung model at a variety of physiologic settings with the simple, the nonrebreathing, and the Venturi-type oxygen masks with different air supply rates.

METHODS

Masks

Three different types of commonly used oxygen masks were used: a simple oxygen mask, a

nonrebreathing mask, and a Venturi-type mask (all from Salter Labs, Arvin, CA).

Lung model and smoke generator

A Laerdal airway management trainer with an artificial lung model (INGMar Medical Adult/Pediatric Demonstration Lung Model; IngMar Medical, Ltd, Pittsburgh, PA) was used to simulate human respiration. A smoke generator (CONCEPT Colt 4 Basic Smoke Generator, 1.1 kW, 220V/50 Hz; Concept Smoke Systems, Maidenhead, Berks, UK) was used to inject smoke into the left lung of the Laerdal trainer, such that the smoke mixed with the inhaled and exhaled oxygen that was supplied at different flow rates. This is a portable smoke gun that produces a persistent, dense smoke, ideal for smoke visualization. The smoke source is canister oil, which is safe to humans. The variable airflow was supplied by an oxygen cylinder and could be set to a flow rate of between 1 and 15 liters per minute.

The Laerdal trainer has realistic anatomic features, and the lung model could simulate a spontaneously breathing patient at a variety of settings, including adjustable respiration rates (RR), tidal volumes (TV), and peak flows. Within the limits of the lung model performance, combinations of RR in breaths per minute and TV in liters were chosen to create 3 ''respiratory models,'' each representative of a commonly encountered patient situation (see Table 1).

Environment

A clean room was constructed for the study with the following dimensions: floor space 2 × 2 m, ceiling height 2.4 m. The ventilation was provided by adjustable speed airflow on the ceiling with ventilation windows on at the bottom of the walls in the corners. An airflow meter monitored the ambient airflow. During the study, the air change rate was maintained at 12 air changes per hour, with the room temperature and humidity remaining at a relatively constant 22.3°C and 62%, respectively. Illumination was provided by normal room strip fluorescent lighting, with the model filmed against a black backdrop to enhance the contrast (Fig 1A).

Image capture and smoke dispersal distance estimates

A digital video (DV) camera (Sony DCR-DVD100E) was used to capture the images of exhaled flows from the respiratory model wearing the different masks at different airflow and respiratory model settings (shown in Table 1). The DV images were examined carefully, and only those that showed the exhaled air plumes most visibly are presented here. The images selected for further analysis were saved as high-resolution bitmaps (approximately 760 × 570 pixels) and enlarged in Microsoft Powerpoint (Microsoft Corp, Redmond, WA) to estimate the maximum smoke dispersal distances.

Table 1. Different physiologic settings or "respiratory models" used in this study

Settings	Model 1	Model 2	Model 3
Respiratory rate (breaths/min)	14	24	30
Tidal volume (mL)	500	330	235

The maximum dispersal distance was estimated using the chin-to-chest distance in one direction (measured and real distance *x1* in Fig 1A) of the Laerdal trainer as a scale for estimating the distance traveled in another direction by the visible smoke (measured and real distance *y1* in Fig 1A) in the captured images. To estimate the error in making such distance measurements from the 2-dimensional (2-D) screen images that were enlarged and printed to perform this measurement, the Laerdal trainer was again set up with the 3 types of oxygen masks, with wooden rods. The rods were actually tapered chopsticks, and the pointed ends conveniently allowed their secure insertion into the particularly small exit holes of the simple and nonrebreathing masks. These rods were of known lengths and were positioned to represent approximately the directions of the chin-to-chest (*x1*) and exhaled smoke plume (*y1*) measurements for each mask. These smoke plumes were emitted in a roughly conically shaped space, with the cone apex adjacent to the oxygen mask, and the rod in the *y1* direction was positioned to lie within this space, accordingly. The Laerdal trainer with the mask and attached rods was carefully positioned to be as similar as possible to that of the corresponding captured digital image for the same mask with its exhaled smoke plumes then photographed at a resolution of 1024 × 768 pixels with a digital camera (Canon Ixus II, Canon Inc., Tokyo, Japan).

This was necessary because of the geometric distortion present because of distances x and y not lying in the same direction or the same plane, which was caused by the relative positions of the Laerdal trainer, the camera, and the direction taken by the exhaled smoke plumes (compare Fig 1A and 1B). The distances *x1* and *y1* were measured from enlarged, printed still images taken from the digital film footage for each mask, at each setting (as shown in Fig 1A). Knowing the real length of the rods (real lengths *x2* and *y2* in Fig 1B), the 2 ratios *x1/x2* and *y1/y2* were compared. If these distances had been measured in the same plane and the same direction on the same screen image, then these 2 ratios should be equal. Any difference between the ratios *x1/x2* and *y1/y2* would be due to

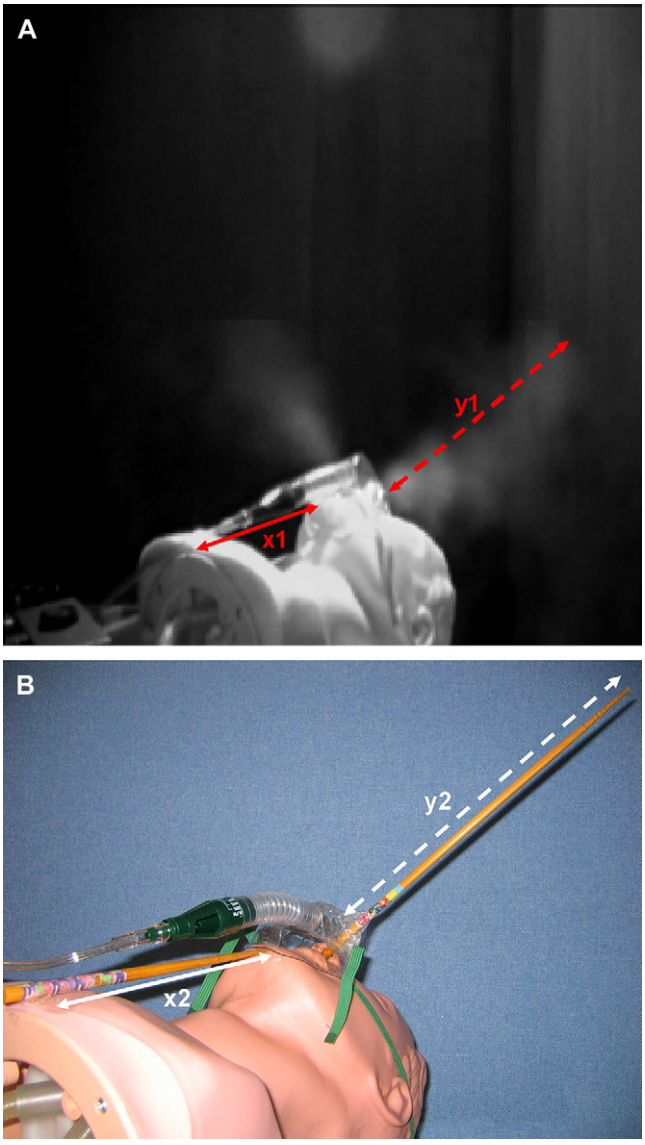

Fig 1. An approximation was made of the maximum visible dispersal distance traveled by the exhaled smoke plume (*y1* in A, shown by dotted line arrow), shown here for the Venturi mask (at 40% O_2, 6 L/min, at respiratory model setting No. 1). This distance had to be estimated, taking into account the geometric distortion due to the different relative positions of the Laerdal trainer, the digital camera, and the direction traveled by the exhaled smoke plume. It was estimated by knowing the real value of the chin-to-chest distance (*x2* in B) on the Laerdal trainer, the measured screen distances of *x1* and *y1* (in A), and the relative error of these measured screen distances, estimated by the ratio (*x1*/*x2*)/(*y1*/*y2*), where the real lengths of the wooden rods, *x2* and *y2*, were known. Note that these ratios *x1*/*x2* and *y1*/*y2* will not be exactly the same because they are measured in different directions and different planes, so they will be at different distances from the camera. It is this difference between ratios *x1*/*x2* and *y1*/*y2* that gives the value of the geometric corrections shown in Table 2.

geometric distortion and give an estimate of the error incurred by measuring and scaling up distances measured from the enlarged, printed, 2-D still images of the exhaled smoke plumes. Therefore, scaled up, real value of *y1* could be estimated as the following:

real *y2* = measured *y1*/(measured *x1*/real *x2*).

Small differences in the position of the Laerdal trainer and the rods between the original captured DV images and the still photographed images would not affect the real distance estimate *y1* too much because the exhaled smoke plumes were conical in shape. As long as the rod representing the *y1* direction did not move too far in any direction, it would probably have remained within the cone of the exhaled smoke plume. Hence, the positioning of the Laerdal trainer with the rods attached to the masks, using a direct eye comparison with the capture DV image, for the still photograph, would still allow a realistic estimate to be made for *y1*.

RESULTS

The most visible exhaled airflows were seen from the simple oxygen mask at oxygen flow rates of 10 L/min and 15 L/min, from the nonrebreathing mask at 8 L/min and 10 L/min, and from the Venturi-type mask at 35% O_2 at 6 L/min and 40% O_2 at 6 L/min. Table 2 shows the estimated distance (with geometric corrections) traveled by the exhaled smoke plumes, based on the scale factor calculated by the following:

real *y2* = measured *y1*/(measured *x1*/real *x2*).

For the simple oxygen mask (at 10 L/min and 15 L/min), the exhaled smoke plumes appeared to travel the least distance. The exhaled smoke plumes from the nonrebreathing mask (at 8 L/min and 10 L/min) were more visible and appeared to travel farther than for the simple oxygen mask. Although there is some overlap with the distances traveled by exhaled smoke plumes from the nonrebreathing mask, overall, those from the Venturi-type mask (as settings of 35% O_2 at 6 L/min and 40% O_2 at 6 L/min) appeared to travel the farthest. Overall, the visible dispersal distances of the exhaled smoke plumes from the simple, the nonrebreathing, and the Venturi-type oxygen masks, at the different oxygen flow rates, with the different respiratory models used in this study (shown in Table 1)

Table 2. Estimated maximum visible smoke dispersal distances, with geometrical correction, at peak of exhalation, for each oxygen mask and for each respiratory model number shown in Table 1

Oxygen mask type	Oxygen flow rate (L/min)	Respiratory model number	Estimated maximum visible dispersal distance ± geometrical correction (cm), (ie, the difference in the ratios *x1*/*x2* and *y1*/*y2*)
Simple	10	1	9.5 ± 0.6 (ie, about 6%)
	10	2	12.5 ± 0.8
	10	3	8.3 ± 0.5
	15	1	11.2 ± 0.7
	15	2	20.7 ± 1.2
	15	3	16.3 ± 1.0
Non-rebreathing	8	1	34.1 ± 3.1 (ie, about 9%)
	8	2	35.8 ± 3.2
	8	3	23.5 ± 2.1
	10	1	24.6 ± 2.2
	10	2	24.6 ± 2.2
	10	3	26.3 ± 2.4
Venturi-type	6 (35% O_2)	1	27.2 ± 1.1 (ie, about 4%)
	6 (35% O_2)	2	33.8 ± 1.4
	6 (35% O_2)	3	27.4 ± 1.1
	6 (40% O_2)	1	39.7 ± 1.6
	6 (40% O_2)	2	39.7 ± 1.6
	6 (40% O_2)	3	26.3 ± 1.1

NOTE. Each of the value of percentages shown are in the last column (6%, 9%, 4%) applies, approximately, to all measurements made for that particular oxygen mask type.

ranged from 0.08 to 0.21 m, 0.23 to 0.36 m, and 0.26 to 0.40 m, respectively. From these distance estimates, respiratory model No. 2 (24 breaths/min, TV 0.33 L) appeared to produce the greatest visible dispersal distance of the exhaled smoke plume.

DISCUSSION

In this study, we have captured and characterized digital images of the exhaled airflows produced from a variety of oxygen masks using an artificial lung model at several physiologic settings. From these results, there seem to be relative differences in the visible distances traveled by the exhaled plumes from each type of mask. Although the relatively higher oxygen flow rates of 10 L/min and 15 L/min used for the simple oxygen mask were not used for the nonrebreathing and the Venturi-type masks, from the results shown in Table 2, it is not unreasonable to assume that the maximum visible dispersal distances (and hence the minimum distances traveled) of the exhaled smoke plume for these latter 2 masks would almost certainly exceed those of the simple oxygen mask at these higher oxygen flow rates. These images should be useful in assessing the infection control risk from potentially infectious exhaled plumes from patients with respiratory symptoms using such masks in health care and community settings.

There are relatively few papers that attempt to visualize exhaled airflows as a potential source of infection. Somogyi et al[17] used a very simple setup, using flash photography, to illustrate the potential dangers of exhaled airflows. Inhaled saline mist was exhaled through 3 commonly used types of oxygen masks, demonstrating that exhaled plumes could spread infectious aerosols over a distance of approximately 1 to 2 head diameters, ie, up to approximately 0.3 m, where an average head diameter is approximately 0.13 to 0.16 m.[23]

Hui et al[18,19] used a 2-D green (527-nm wavelength) laser sheet to illuminate oil-based smoke particles (<1-μm diameter) to illustrate the dispersion of potentially infectious exhaled plumes from a variety of respiratory support devices and procedures, including oxygen masks and noninvasive positive pressure ventilation. From these latter 2 studies, the estimated dispersal distances of exhaled, potentially infectious, air from patients using such respiratory assist devices were in the range of 0.40 to 0.50 m. These studies used a more sophisticated lighting system with monochromatic, coherent laser light-sheet. They also tested a more limited range or a totally different respiratory assistance setup, ie, a simple oxygen mask at 1 respiratory setting (RR = 12 breaths/min; TV = 0.5 L; oxygen flow rate = 4 L/min),[18] and noninvasive positive-pressure ventilation.[19] This present study also differs from those of Hui et al[18,19] in that it was performed in a more typical isolation room environment, with ambient lighting and a background ventilation rate of 12 air changes per hour. The exact effect of the 12 air changes per hour on the extent of the smoke plumes is difficult to quantify, although their dispersal patterns as shown here may be more representative of those seen in isolation rooms commonly used for patients suspected to be infected with respiratory pathogens of higher morbidity/mortality.

It is interesting that the extent of visible smoke dispersion recorded is similar in all these setups (up to a maximum of approximately 0.4 m from the patient), which may well be due to the different lighting conditions used, particularly between this present study and that of Hui et al.[18,19] With the more intense laser-sheet lighting used by Hui et al, it is likely that further distances would have been recorded for the limits of visible smoke dispersal, at the higher oxygen flow rates used in this study. Hence, the 0.4-m distance estimated here can only be considered a lower limit for the extent of any ''nosocomial hazard zone,'' as defined by the visible dispersal limits of the smoke tracer used here.

Although current guidelines for the infection control of aerosol transmission is mainly limited to 3 pathogens

(measles, chickenpox, and tuberculosis),[2,24] other infectious agents such as influenza and whooping cough may be just as transmissible in certain situations, as suggested by previous relatively high estimates of their basic reproductive numbers (R_0) of approximately 2 to 20 (for influenza) and 15 to 17 (for whooping cough).[2] These guidelines and R_0 values apply to natural methods of dissemination, such as normal breathing, coughing, sneezing, and talking. However, when respiratory assist devices are used and infectious exhaled air is mixed and expelled with oxygen/air at high flow rates, the potential for increased transmissibility is evident.

It is important to recognize the limitations of this visualization approach. The visible boundaries of exhaled flows can only be a *guide* to the real behavior of infectious droplets in exhaled air. Although Hui et al[18,19] suggested upper limits of exhaled-plume distances as possible safety zones, some of the more distantly dispersed particles may not be visible in their image capture systems. Somogyi et al[17] presented their results in a slightly different manner by stating that the visible cloud (or smoke), in fact, indicates the *minimum* distance traveled by the exhaled air, which may be a more cautious approach that can be used to interpret the results presented in this study. Hence, from this study, those of Hui et al,[18,19] and to a lesser extent that of Somoygi et al,[17] there is a suggestion of a *minimum* baseline ''nosocomial hazard zone'' extending to *at least* 0.4 m away from patients using such respiratory support devices. It is likely to extend farther than this, but this could not be quantified from this study. Such a ''nosocomial hazard zone'' may well increase in size when the patient coughs or sneezes. This could not be examined using the same respiratory model used in this study (there is no cough function) but is certainly worthy of further investigation using other models, eg, perhaps using human volunteers.

With concerns for a possible influenza pandemic, aerosol transmission infection control is becoming more important. Although direct contact transmission predominates as the main route of nosocomial transmission for most pathogens, the relevance of long-distance transmission has become a concern in the design of new hospitals. This has led to an increased number of single-bed, negative pressure isolation rooms, as well as greater distances between beds in such new facilities.[25] Since the 2003 SARS outbreaks, the modeling of airflows in health care institutions has been performed in a variety of ways and on different scales by both engineers[7-9,26-29] and physicians.[3,5,6,12,17-19] Studies assessing the effectiveness of personal protective equipment, such as masks, have also been performed.[30]

With influenza, the relative risk from airborne of contact transmission is still being hotly debated, and even existing infection control guidelines have been questioned in this regard.[16] The airborne route of influenza has been well documented,[31-35] so why do some guidelines still treat influenza as a short-range rather than a long-range airborne disease?[16] Perhaps the most useful debate has been published by the UK Health Protection Agency's Guidance for Pandemic Influenza that comprehensively summarizes the evidence for the different transmission routes of influenza. It still concludes, however, that influenza is mostly transmitted by large droplets and direct contact.[15] Tellier[16] goes one step further and presents a convincing argument as to why influenza should be considered as a true airborne infection and recommends N95 respirators as the minimum level of personal protective equipment for the purposes of pandemic influenza planning.

These debates notwithstanding, the use of respiratory assist devices, similar to those shown in this study, on the basis of the physics alone, has the potential to increase the distance over which influenza and other aerosol-transmitted infections can be naturally transmitted,[2] thus elevating its potential transmission risk to that of a true airborne disease in such situations.

Most nosocomial and community-acquired respiratory infections are mild and unlikely to cause severe morbidity or mortality during a nonpandemic period. However, when a new respiratory pathogen arises, with the potential to cause high morbidity and mortality, eg, SARS and more recently avian H5N1 or possibly some other future pandemic influenza strain, this baseline data should be useful in reducing nosocomial transmission and enhancing health care workers' awareness of the risks posed by the use of such respiratory assist devices. In addition, it is known that, unlike SARS-associated coronavirus, influenza may be presymptomatically transmissible.[36,37] Hence, there is a convincing argument for all staff working in the immediate vicinity, ie, within a zone of 0.4 m, of such patients, to be wearing N95 masks as their minimum personal protective equipment during an influenza pandemic or when dealing with any other respiratory pathogen with the potential to cause high morbidity and mortality.

References

1. Li Y, Leung GM, Tang JW, Yang X, Chao CY, Lin JZ, et al. Role of ventilation in airborne transmission of infectious agents in the built environment: a multidisciplinary systematic review. Indoor Air 2007;17:2-18.
2. Tang JW, Li Y, Eames I, Chan PK, Ridgway GL. Factors involved in the aerosol transmission of infection and control of ventilation in healthcare premises. J Hosp Infect 2006;64:100-14.
3. Wong TW, Lee CK, Tam W, Lau JT, Yu TS, Lui SF, et al. Cluster of SARS among medical students exposed to single patient, Hong Kong. Emerg Infect Dis 2004;10:269-76.

4. Olsen SJ, Chang HL, Cheung TY, Tang AF, Fisk TL, Ooi SP, et al. Transmission of the severe acute respiratory syndrome on aircraft. N Engl J Med 2003;349:2416-22.
5. Yu IT, Li Y, Wong TW, Tam W, Chan AT, Lee JH, et al. Evidence of airborne transmission of the severe acute respiratory syndrome virus. N Engl J Med 2004;350:1731-9.
6. Yu IT, Wong TW, Chiu YL, Lee N, Li Y. Temporal-spatial analysis of severe acute respiratory syndrome among hospital inpatients. Clin Infect Dis 2005;40:1237-43.
7. Wang B, Zhang A, Sun JL, Liu H, Hu J, Xu LX. Study of SARS transmission via liquid droplets in air. J Biomech Eng 2005;127:32-8.
8. Li Y, Huang X, Yu IT, Wong TW, Qian H. Role of air distribution in SARS transmission during the largest nosocomial outbreak in Hong Kong. Indoor Air 2005;15:83-95.
9. Li Y, Duan S, Yu IT, Wong TW. Multi-zone modeling of probable SARS virus transmission by airflow between flats in Block E. Amoy Gardens. Indoor Air 2005;15:96-111.
10. Xiao WJ, Wang ML, Wei W, Wang J, Zhao JJ, Yi B, et al. Detection of SARS-CoV and RNA on aerosol samples from SARS-patients admitted to hospital. Zhonghua Liu Xing Bing Xue Za Zhi 2004;25: 882-5.
11. Booth TF, Kournikakis B, Bastien N, Kobasa D, Stadnyk L, Li Y, et al. Detection of airborne severe acute respiratory syndrome (SARS) coronavirus and environmental contamination in SARS outbreak units. J Infect Dis 2005;191:1472-7.
12. Tang JW, Eames I, Li Y, Taha YA, Wilson P, Bellingan G, et al. Door-opening motion can potentially lead to a transient breakdown in negative-pressure isolation conditions: the importance of vorticity and buoyancy airflows. J Hosp Infect 2005;61:283-6.
13. Fennelly KP, Martyny JW, Fulton KE, Orme IM, Cave DM, Heifets LB. Cough-generated aerosols of Mycobacterium tuberculosis: a new method to study infectiousness. Am J Respir Crit Care Med 2004; 169:604-9.
14. Hayden F, Croisier A. Transmission of avian influenza viruses to and between humans. J Infect Dis 2005;192:1311-4.
15. HPA. Health Protection Agency. Guidance for pandemic influenza: infection control in hospitals and primary care settings. Department of Health, United Kingdom; October 2005. p. 68.
16. Tellier R. Review of aerosol transmission of influenza A virus. Emerg Infect Dis 2006;12:1657-62.
17. Somogyi R, Vesely AE, Azami T, Preiss D, Fisher J, Correia J, et al. Dispersal of respiratory droplets with open vs closed oxygen delivery masks: implications for the transmission of severe acute respiratory syndrome. Chest 2004;125:1155-7.
18. Hui DS, Ip M, Tang JW, Wong AL, Chan MT, Hall SD, et al. Airflows around oxygen masks: a potential source of infection? Chest 2006; 130:822-6.
19. Hui DS, Hall SD, Chan MT, Chow BK, Tsou JY, Joynt GM, et al. Noninvasive positive-pressure ventilation: an experimental model to assess air and particle dispersion. Chest 2006;130:730-40.
20. Soo SL. Fluid dynamics of multiphase systems. Toronto: Blaisdell Publishing Company; 1967.
21. Hall SD. An investigation of the turbulent backward facing step flow with the addition of a charged particle phase and electrostatic forces. PhD dissertation. University of New South Wales: Sydney, NSW, Australia; 2001.
22. Nicas M, Nazaroff WW, Hubbard A. Toward understanding the risk of secondary airborne infection: emission of respirable pathogens. J Occup Environ Hyg 2005;2:143-54.
23. Anderson V. Comparisons of peak SAR levels in concentric sphere head models of children and adults for irradiation by a dipole at 900 MHz. Phys Med Biol 2003;48:3263-75.
24. CDC. Centers for Disease Control and Prevention. Guidelines for environmental infection control in health-care facilities. Mor Mortal Wkly Rep 2003;52(RR-10):1-42.
25. Wilson AP, Ridgway GL. Reducing hospital-acquired infection by design: the new University College London Hospital. J Hosp Infect 2006;62:264-9.
26. Qian H, Li Y, Nielsen PV, Hyldgaard CE, Wong TW, Chwang AT. Dispersion of exhaled droplet nuclei in a two-bed hospital ward with three different ventilation systems. Indoor Air 2006;16:111-28.
27. Brohus H, Balling KD, Jeppesen D. Influence of movements on contaminant transport in an operating room. Indoor Air 2006;16:356-72.
28. Kao PH, Yang RJ. Virus diffusion in isolation rooms. J Hosp Infect 2006; 62:338-45.
29. Noakes CJ, Beggs CB, Sleigh PA, Kerr KG. Modelling the transmission of airborne infections in enclosed spaces. Epidemiol Infect 2006;134: 1082-91.
30. Derrick JL, Li PT, Tang SP, Gomersall CD. Protecting staff against airborne viral particles: in vivo efficiency of laser masks. J Hosp Infect 2006;64:278-81.
31. Moser MR, Bender TR, Margolis HS, Noble GR, Kendal AP, Ritter DG. An outbreak of influenza aboard a commercial airliner. Am J Epidemiol 1979;110:1-6.
32. Goldmann DA. Transmission of viral respiratory infections in the home. Pediatr Infect Dis J 2000;19(Suppl 10):S97-102.
33. Goldmann DA. Epidemiology and prevention of pediatric viral respiratory infections in health-care institutions. Emerg Infect Dis 2001;7: 249-53.
34. Salgado CD, Farr BM, Hall KK, Hayden FG. Influenza in the acute hospital setting. Lancet Infect Dis 2002;2:145-55.
35. Bridges CB, Kuehnert MJ, Hall CB. Transmission of influenza: implications for control in health care settings. Clin Infect Dis 2003;37: 1094-101.
36. Fraser C, Riley S, Anderson RM, Ferguson NM. Factors that make an infectious disease outbreak controllable. Proc Natl Acad Sci U S A 2004;101:6146-51.
37. Wu JT, Riley S, Fraser C, Leung GM. Reducing the impact of the next influenza pandemic using household-based public health interventions. PLoS Med 2006;3:e361.